

Iterative Learning enhanced Integral Terminal Sliding Mode Control for Precision Motion Systems

Zhao Feng¹, Jie Ling², Feng Wan¹, Zhi-Xin Yang³

1. Department of Electrical and Computer Engineering, University of Macau, Macao, P. R. China

E-mail: zhaofeng@um.edu.mo; fwan@um.edu.mo; zxyang@um.edu.mo

2. College of Mechanical & Electrical Engineering, Nanjing University of Aeronautics and Astronautics, Nanjing 210016, P. R. China

E-mail: meejing@nuaa.edu.cn

3. State Key Laboratory of Internet of Things for Smart City and Department of Electromechanical Engineering, University of Macau, Macao, P. R. China

E-mail: zxyang@um.edu.mo

Abstract:

The rapid development and applications of precision motion systems pose a great challenge on tracking performance improvement to complete various industrial or scientific tasks. In this paper, an iterative learning enhanced integral terminal sliding mode control (IL-ITSMC) is developed to further enhance the performance of such systems under repetitive trajectory and disturbance. For the generally used second-order model in precision motion systems, an integral terminal sliding surface is utilized to improve the steady-state performance and robustness to unexpected disturbance. A novel reaching law is also designed to realize the finite-time convergence of the sliding surface. In addition, an iterative learning law is proposed based on the sliding surface to compensate the repetitive term through updating the feedforward control input iteratively. The stability in time domain and convergence in iterative domain are proven theoretically based on the well-known Lyapunov theory, respectively. The simulation results on a piezo-actuated stage with hysteresis nonlinearity demonstrate that the proposed IL-ITSMC achieves the best tracking performance through comparisons, and the convergence speed is improved significantly in comparison with ITSMC with traditional P-type ILC (PIL-ITSMC) for a 10 Hz sinusoidal repetitive trajectory.

Key Words: Precision Motion Tracking, Sliding Mode Control, Iterative Learning Control

1 Introduction

Precision motion systems play a vital role in modern industrial and scientific fields [1], where various motion systems are utilized to arrive the desired points or track specific trajectories. Among these, piezoelectric-actuated devices have been widely designed and used dedicated to achieve nanometer or sub-nanometer precision [2]. However, the inherent nonlinearities, such as hysteresis and friction in such systems deteriorate the overall performances significantly [3],[4]. Hence, a well-designed controller could make a great improvement on the tracking precision.

The compensation of nonlinearities can be mitigated by the developed inverse hysteresis or friction models [4],[5]. Although various mathematical models are constructed to describe the nonlinearities, the accurate compensation needs to identify lots of parameters and the processes are time-consuming in the view of practical implementation. In order to avoid the complex identification, the feedback controllers can be utilized to enhance the disturbance rejection ability by treating the nonlinearities as input disturbances [6],[7].

The robust control technology can provide the significant improvement of tracking performance and disturbance suppression. Sliding mode control (SMC) is one of the effective and simple methodologies through driving the sliding surface to the origin with strong robustness to uncertainties and disturbances [8],[9]. The conventional sliding

surfaces are proportional-derivative (PD) or proportional-integral-derivative (PID) types, which can only realize convergence with infinite time. In order to increase the convergence speed, the nonlinear terminal sliding surface that contains fractional-order term of error is developed to realize finite-time convergence [10],[11]. Furthermore, to further improve the tracking performance, the integral term should be included in the control scheme [12]. The integral type sliding surface can obtain better steady-state performance, fast response, eliminate the reaching phase and smooth the control law [13]. However, the key disadvantage of SMC is the phenomenon of high-frequency oscillation due to the switching term in the control law. To retain closed-loop stability, the assigned large switching gain will generate large and chattering control force that may even damage the actuator. Moreover, although SMC can track arbitrary trajectories, the tracking precision is still limited by its pure feedback scheme, which requires the integration with the feedforward control to pursue better performance.

In some applications, such as lithography machine [14], atomic force microscopy [15], the trajectory is repetitive for the motion systems. Therefore, iterative learning control (ILC) is a natural solution to further improve the precision. In conventional ILC, the tracking errors are compensated by learning from the previous iterations and updating the control signal for the next iteration [16],[17]. Based on the previous cycle information, the control input can be calculated by either the norm-optimal method [18] or the frequency-domain approach [19]. Inversion-based ILC in frequency domain is a popular method for practical implementation with the merits of lower complexity and fast convergence [20]. However, an accurate model should be ob-

This work is supported by the Science and Technology Development Fund, Macau SAR (Grant no. 0018/2019/AKP, 0008/2019/AGJ, and SKL-IOTSC-2021-2023), in part by the Ministry of Science and Technology of China under Grant 2019YFB1600700, in part by the University of Macau (Grant No.: MYRG2018-00248-FST and MYRG2019-0137-FST), and in part by the University of Macau under UM Macao Talent Programme (UMMTP-2020-01).

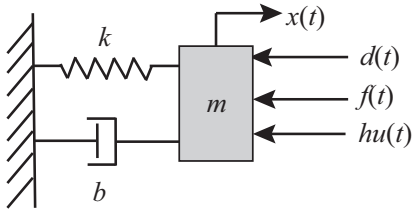


Fig. 1: A diagram for the mathematical model of precision motion systems.

tained or identified in order to achieve sufficient precision. It should be noted that P-type or PD-type ILC can avoid accurate modeling, but the convergence rate is low so that lots of iterations should be conducted on the plant. Furthermore, the non-repetitive disturbance cannot be compensated by the updated ILC signal, which is commonly in piezoelectric-actuated device, like hysteresis and friction depended on the system states. Therefore, the suppression on such disturbance should be also taken into consideration when designing ILC.

Motivated by aforementioned important issues, an iterative learning enhanced integral terminal sliding mode control (IL-ITSMC) is proposed for precision motion systems suffering from repetitive disturbance and nonlinearities. An integral terminal sliding surface is used to achieve better performance and finite-time convergence, and a sliding surface based iterative learning law is developed to estimate and compensate the repetitive disturbances so that the chattering is alleviated for a small switching gain. The stability in time-domain and convergence in iterative domain are proven theoretically based on the well-known Lyapunov theory, respectively. Furthermore, the simulations on a piezo-actuated stage with hysteresis nonlinearity are conducted to demonstrate the performance improvement in comparison with integral terminal sliding mode control (ITSMC) and ITSMC with traditional P-type ILC (PIL-ITSMC). Being different from the conventional ILC using tracking error to update control input, the sliding surface is used in this paper, and due to the integration with ITSMC, the impact of non-repetitive error is reduced significantly so that the convergence speed is also improved.

The rest of this paper is structured as follows. Model description and assumptions are presented Section 2. The detailed design and stability of the controller are given in Section 3. The simulation results are shown in Section 4, and Section 5 gives the conclusion.

2 Preliminaries

In this paper, a commonly used single-input-single-output (SISO) second-order system is utilized to describe the precision motion systems [11],[12], which is given by

$$m\ddot{x}(t) + b\dot{x}(t) + kx(t) = hu(t) + f(t) + d(t), \quad (1)$$

where $x(t)$ is output position, $\dot{x}(t)$ and $\ddot{x}(t)$ are the velocity and acceleration. m, b, k are the effective mass, damping and stiffness coefficients. The input is denoted as $u(t)$ which is driven by the electromechanical ratio h . $f(t)$ and $d(t)$ are the repetitive and non-repetitive disturbances, respectively. The diagram for the mathematical model of precision motion systems is demonstrated in Fig. 1.

Assumption 1: The desired position $x_d(t)$ and disturbance $f(t)$ are repetitive on a finite time interval $[0, T]$, i.e.

$$x_d(t) = x_{d,i}(t) = x_{d,i+1}(t), f(t) = f_i(t) = f_{i+1}(t), \quad (2)$$

where $i \in \{1, 2, 3, \dots, K\}$ indicates the iterative number with maximal iteration K . Therefore, $x_{d,i}(t)$ and $f_i(t)$ suffer from the identical initial conditions for every iteration.

Assumption 2: The term $d(t)$ is bounded during all the iterations and satisfies the following conditions,

$$|d_i(t)| \leq D \quad (3)$$

In addition, the following lemmas will be useful for the controller design.

Lemma 1: (see [21]) The origin of the following system is a globally finite-time-stable equilibrium:

$$\begin{cases} \dot{x}_1 = x_2 \\ \dot{x}_2 = -k_2 \text{sgn}(x_2)|x_2|^\gamma - k_1 \text{sgn}(x_1)|x_1|^{\frac{\gamma}{2-\gamma}} \end{cases}, \quad (4)$$

where k_1, k_2 are positive constants, chosen such that the polynomial $r^2 + k_2 r + k_1$ is Hurwitz, and $0 < \gamma < 1$.

Lemma 2: (see [22]) An extended Lyapunov description V of finite-time stability can be given with the form of fast terminal sliding mode as

$$\dot{V} + a_1 V + a_2 V^{a_3} \leq 0, a_1 > 0, a_2 > 0, 0 < a_3 < 1 \quad (5)$$

and the settling time with initial state V_0 can be given by

$$t_r \leq \frac{1}{a_1(1-a_3)} \ln \frac{a_1 V_0^{1-a_3} + a_2}{a_2} \quad (6)$$

3 Iterative Learning Enhanced Integral Terminal Sliding Mode Control

3.1 Controller Design

The goal in this paper is to achieve the precision tracking of the system (1), i.e. to minimize the tracking error $e_i(x) = x_i(t) - x_d(t)$ through iterations. Firstly, we define the following integral terminal sliding surface at iteration i as

$$s_i(t) = \dot{e}_i(t) + \int_0^t k_2 \text{sgn}(\dot{e}_i(\tau)) |\dot{e}_i(\tau)|^\gamma + k_1 \text{sgn}(e_i(\tau)) |e_i(\tau)|^{\frac{\gamma}{2-\gamma}} d\tau. \quad (7)$$

It should be noted that although the sliding manifold contains the switching term $\text{sgn}(\cdot)$, the sliding surface $s_i(t)$ is continuous and differentiable. Thus, the derivative of $s_i(t)$ with respect to time t yields

$$\dot{s}_i(t) = \ddot{e}_i(t) + k_2 \text{sgn}(\dot{e}_i(t)) |\dot{e}_i(t)|^\gamma + k_1 \text{sgn}(e_i(t)) |e_i(t)|^{\frac{\gamma}{2-\gamma}}. \quad (8)$$

With the equation $\ddot{e}_i(t) = \ddot{x}_d - \ddot{x}_i(t)$ and (1), through making $\dot{s}_i(t) = 0$ and neglecting unknown term $d_i(t)$, the equivalent control input is calculated as

$$u_i^{eq} = \frac{1}{h} (b\dot{x}_i(t) + kx_i(t)) + \frac{m}{h} (\ddot{x}_d - k_2 \text{sgn}(\dot{e}_i(t)) |\dot{e}_i(t)|^\gamma - k_1 \text{sgn}(e_i(t)) |e_i(t)|^{\frac{\gamma}{2-\gamma}}). \quad (9)$$

Furthermore, in order to achieve fast convergence to the sliding surface and retain robustness to disturbance $d_i(t)$, the following reaching law is designed in this paper as

$$u_i^{sw}(t) = -\frac{1}{h}v_i(t) = -\frac{1}{h}(\alpha_1 s_i(t) + \alpha_2 \text{sgn}(s_i(t))|s_i(t)|^p + k_s \text{sgn}(s_i(t))) \quad (10)$$

where α_1, α_2, k_s , and $0 < p < 1$ are positive constants.

Besides, the repetitive disturbance $f_i(t)$ is estimated and compensated by the following update law as

$$\begin{aligned} u_i^{il}(t) &= -\frac{1}{h}\hat{f}_i(t) \\ \hat{f}_i(t) &= \hat{f}_{i-1}(t) + (\beta_1 s_i(t) + \beta_2 \text{sgn}(s_i(t))|s_i(t)|^{p-1} + \beta_3 \text{sgn}(s_i(t))) \end{aligned} \quad (11)$$

where $\beta_1, \beta_2, \beta_3$ are positive constants, and $\hat{f}_i(t)$ is the estimated repetitive disturbance. Therefore, the proposed IL-ITSMC is given by

$$u_i(t) = u_i^{eq}(t) + u_i^{il}(t) + u_i^{sw}(t). \quad (12)$$

It is evident that the proposed method utilizes the sliding surface to update the iterative learning law so that the repetitive part in $s_i(t)$, including repetitive errors and disturbance can be compensated.

3.2 Stability and Convergence Analysis

The stability and convergence analysis are given in this section. In what follows, the time variable t is omitted for brief to simplify the writing of the equations, and the integral symbol is expressed briefly as $\int_0^t X(\tau) d\tau = \int X$.

Theorem 1 (Stability in Time Domain): For the system described by (1) with the control law (12), the sliding function s_i as well as error e_i will converge to zero in finite time if the parameter k_s is satisfied by

$$k_s \geq |f - \hat{f}_i + d_i| \quad (13)$$

Proof: The Lyapunov function candidate is given as

$$V_i^{td} = \frac{1}{2}s_i^2, \quad (14)$$

and its derivative with respect to time is calculated as

$$\dot{V}_i^{td} = s_i \dot{s}_i. \quad (15)$$

Substituting the control law into (8) yields

$$\begin{aligned} \dot{s}_i &= \frac{1}{m}(hu_i - b\dot{x}_i - kx_i + f_i + d_i) - \ddot{x}_d + \\ & k_2 \text{sgn}(\dot{e}_i)|\dot{e}_i|^\gamma + k_1 \text{sgn}(e_i)|e_i|^{\frac{\gamma}{2-\gamma}} \\ &= \frac{1}{m}(-\hat{f}_i + f_i + d_i + v_i). \end{aligned} \quad (16)$$

Taking (16) into (15), we have

$$\begin{aligned} \dot{V}_i^{td} &= \frac{1}{m}s_i(-\hat{f}_i + f_i + d_i + v_i) \\ &= \frac{1}{m}[s_i(-\hat{f}_i + f_i + d_i) - k_s|s_i|] - \\ & \frac{1}{m}(\alpha_1 s_i^2 + \alpha_2 |s_i|^{p+1}). \end{aligned} \quad (17)$$

From the condition (13) and Lyapunov function (14), it is obtained that

$$\dot{V}_i^{td} + \frac{2\alpha_1}{m}V_i^{td} + \frac{\sqrt{2}\alpha_2}{m}(V_i^{td})^{\frac{p+1}{2}} \leq 0. \quad (18)$$

Therefore, according to Lemma 2, the sliding surface will converge to the origin in finite time as

$$t_r \leq \frac{m}{\alpha_1(1-p)} \ln \frac{2\alpha_1(V_i^{td}(0))^{\frac{1-p}{2}} + \sqrt{2}\alpha_2}{\sqrt{2}\alpha_2}. \quad (19)$$

After the time t_r , s_i will converge to zero so that $\dot{s}_i \rightarrow 0$. Therefore, with Lemma 1, the error is globally finite-time-stable to the equilibrium point $e_i = 0$. The proof is completed. ■

From the above analysis, it is concluded that the stability in the time domain is determined by the iteration approximation error $\tilde{f}_i = f - \hat{f}_i$. Next, the convergence in iterative domain is given.

Theorem 2 (Convergence in Iterative Domain): For the system described by (1) with the control law (12), it is guaranteed that the system output errors will asymptotically converge to zero over $[0, T]$ when the iteration number approaches infinity if $k_s > D$.

Proof: The Lyapunov function candidate in the i th iteration is selected as

$$V_i = V_i^1 + V_i^2 + V_i^3 + V_i^4, \quad (20)$$

where

$$\begin{aligned} V_i^1 &= \frac{1}{2}m\beta_1 s_i^2, V_i^2 = \frac{\beta_2}{p}|s_i|^p, \\ V_i^3 &= \beta_3|s_i|, V_i^4 = \frac{1}{2} \int \tilde{f}_i^2. \end{aligned} \quad (21)$$

(i) The difference of V_i^1 between i and $i-1$ iteration is deduced as

$$\begin{aligned} \Delta V_i^1 &= \frac{1}{2}m\beta_1 s_i^2 - \frac{1}{2}m\beta_1 s_{i-1}^2 \\ &= \beta_1 \int s_i(-\hat{f}_i + f + d_i + v_i) - \frac{1}{2}m\beta_1 s_{i-1}^2. \end{aligned} \quad (22)$$

According to the control law, we have

$$\begin{aligned} \Delta V_i^1 &= \int s_i(\tilde{f}_i + d_i + v_i) - \frac{m}{2}\beta_1 s_{i-1}^2 \\ &= \beta_1 \int s_i \tilde{f}_i + \beta_1 \int s_i d_i + \beta_1 \int s_i(-\alpha_1 s_i - \\ & \alpha_2 \text{sgn}(s_i)|s_i|^p - k_s \text{sgn}(s_i)) - \frac{m}{2}\beta_1 s_{i-1}^2 \\ &= \beta_1 \int s_i \tilde{f}_i + \beta_1 \int (s_i d_i - \alpha_1 \beta_1 s_i^2 - \\ & \alpha_2 \beta_1 |s_i|^{p+1}) - k_s \beta_1 \int |s_i| - \frac{m}{2}\beta_1 s_{i-1}^2. \end{aligned} \quad (23)$$

(ii) The difference of V_i^2 between i and $i-1$ iteration is deduced as

$$\Delta V_i^2 = \frac{\beta_2}{p}|s_i|^p - \frac{\beta_2}{p}|s_{i-1}|^p. \quad (24)$$

It should be noted that the following equation holds,

$$\frac{d}{dt}|s_i|^p = p|s_i|^{p-1} \text{sgn}(s_i) \dot{s}_i. \quad (25)$$

Therefore, the equation (24) becomes

$$\begin{aligned}
\Delta V_i^2 &= \beta_2 \int |s_i|^{p-1} \text{sgn}(s_i) \dot{s}_i - p^{-1} \beta_2 |s_{i-1}|^p \\
&= \beta_2 \int |s_i|^{p-1} \text{sgn}(s_i) (\tilde{f}_i + d_i + v_i) - p^{-1} \beta_2 |s_i|^p \\
&= \beta_2 \int |s_i|^{p-1} \text{sgn}(s_i) \tilde{f}_i + \beta_2 \int |s_i|^{p-1} \text{sgn}(s_i) \\
&\quad (d_i - k_s \text{sgn}(s_i)) - \beta_2 \int (\alpha_1 |s_i|^p + \alpha_2 |s_i|^{2p-1}) - \\
&\quad p^{-1} \beta_2 |s_{i-1}|^p.
\end{aligned} \tag{26}$$

(iii) The difference of V_i^3 between i and $i-1$ iteration is deduced as

$$\begin{aligned}
\Delta V_i^3 &= \beta_3 |s_i| - \beta_3 |s_{i-1}| \\
&= \beta_3 \int \text{sgn}(s_i) \dot{s}_i - \beta_3 |s_{i-1}| \\
&= \beta_3 \int \text{sgn}(s_i) (\tilde{f}_i + d_i + v_i) - \beta_3 |s_{i-1}| \\
&= \beta_3 \int \text{sgn}(s_i) \tilde{f}_i + \beta_3 \int \text{sgn}(s_i) (d_i - k_s \text{sgn}(s_i)) - \\
&\quad \beta_3 \int (-\alpha_1 |s_i| + \alpha_2 |s_i|^{p+1}) - \beta_3 |s_{i-1}|.
\end{aligned} \tag{27}$$

(iv) The difference of V_i^4 between i and $i-1$ iteration is deduced as

$$\Delta V_i^4 = \frac{1}{2} \int (\tilde{f}_i^2 - \tilde{f}_{i-1}^2). \tag{28}$$

According to Assumption 1, the following equation is obtained that

$$\begin{aligned}
(\tilde{f}_i^2 - \tilde{f}_{i-1}^2) &= (f - \hat{f}_i)^2 - (f - \hat{f}_{i-1})^2 \\
&= (f - \hat{f}_i)^T (f - \hat{f}_i) - (f - \hat{f}_{i-1})^T (f - \hat{f}_{i-1}) \\
&= (\hat{f}_{i-1} - \hat{f}_i) (2(f - \hat{f}_i) + (\hat{f}_i - \hat{f}_{i-1})) \\
&= (\hat{f}_i - \hat{f}_{i-1}) (2\hat{f}_i - 2f - \hat{f}_i + \hat{f}_{i-1}) \\
&= 2(\hat{f}_i - \hat{f}_{i-1}) (\hat{f}_i - f) - \\
&\quad (\hat{f}_i - \hat{f}_{i-1}) (\hat{f}_i - \hat{f}_{i-1})
\end{aligned} \tag{29}$$

Taking it into (28) yields

$$\begin{aligned}
\Delta V_i^4 &= \int (\hat{f}_i - \hat{f}_{i-1}) (\hat{f}_i - f) - \\
&\quad \frac{1}{2} \int (\beta_1 s_i + \beta_2 \text{sgn}(s_i) |s_i|^p + \beta_3 \text{sgn}(s_i))^2 \\
&= \int (\beta_1 s_i + \beta_2 \text{sgn}(s_i) |s_i|^p + \beta_3 \text{sgn}(s_i)) \tilde{f}_i - \\
&\quad \frac{1}{2} \int (\beta_1 s_i + \beta_2 \text{sgn}(s_i) |s_i|^p + \beta_3 \text{sgn}(s_i))^2 \\
&= -\beta_1 \int s_i \tilde{f}_i - \beta_2 \int \text{sgn}(s_i) |s_i|^p \tilde{f}_i - \\
&\quad \beta_3 \int \text{sgn}(s_i) \tilde{f}_i - \frac{1}{2} \int (\beta_1 s_i + \beta_2 \text{sgn}(s_i) |s_i|^p + \\
&\quad \beta_3 \text{sgn}(s_i))^2.
\end{aligned} \tag{30}$$

Table 1: Model Parameters of the Precision Motion System

Parameter	Value
m	1.8×10^{-3}
b	3.3×10^{-3}
k	1.1639×10^{-3}
ψ	2.4373×10^{-5}
h_1	0.1947
h_2	3.3626
h_3	-2.8526

Based on the above results, the difference of the Lyapunov function V_i is calculated as

$$\begin{aligned}
\Delta V_i &= \Delta V_i^1 + \Delta V_i^2 + \Delta V_i^3 + \Delta V_i^4 \\
&\leq -\beta_1 \int (-s_i d_i + k_s |s_i|) - \beta_2 \int |s_i|^{p-1} \text{sgn}(s_i) \\
&\quad (-d_i + k_s \text{sgn}(s_i)) - \beta_3 \int \text{sgn}(s_i) (-d_i + k_s \text{sgn}(s_i)).
\end{aligned} \tag{31}$$

It is indicated that if $k_s > D$ is satisfied, $\Delta V_i < 0$ is achieved. This result concludes that the Lyapunov function V_i is convergent. Thus, the sliding surface will be driven to zero during iteration so that e_i is minimized. The proof of Theorem 2 is completed. ■

Remark 1: From Theorem 1 and Theorem 2, it is clear that the chattering phenomenon is alleviated because the repetitive term is compensated by the iterative learning law so that the switching gain can be chosen relatively smaller than traditional ITSMC.

Remark 2: The integration of ILC makes further improvement of pure feedback controllers for repetitive trajectory and disturbance. Moreover, the proposed method also makes use of the robustness to non-repetitive disturbance of ITSMC to minimize the impact on ILC so that the convergence speed is improved significantly.

4 Simulation Results

In this section, a piezo-actuated nanopositioning system is used to test the performance of the proposed control method. The model with hysteresis described by Bouc-Wen model is given as

$$\begin{aligned}
m\ddot{x}(t) + b\dot{x}(t) + kx(t) &= k[\psi u(t) - H(t)], \\
\dot{H}(t) &= h_1 \psi \dot{u}(t) - h_2 |\dot{u}(t)| H(t) - h_3 \dot{u}(t) |H(t)|,
\end{aligned} \tag{32}$$

where the system parameters are listed in Tab. 1.

To illustrate the performance of the proposed IL-ITSMC, another two controllers are developed for comparison through simulations. The first controller is the baseline ITSMC, the control law is given as

$$u^1(t) = u^{eq}(t) + u^{sw}(t). \tag{33}$$

It is evident that the controller is conducted without the iterative process. The second controller is the commonly used P-type ILC with ITSMC, i.e. PIL-ITSMC, the control input is calculated by the following equations,

$$u^2(t) = u_i^{eq}(t) + u_i^{sw}(t) + u_i^{pil}(t), \tag{34}$$

where the P-type update law is given by

$$u_i^{pil}(t) = u_{i-1}^{pil}(t) - k_p e_i(t). \tag{35}$$

Table 2: Control Parameters of the Controllers

Parameter	Value	Parameter	Value
k_1	2.5×10^7	k_s	0.1
k_2	200	β_1	1.8
γ	0.99	β_2	0.001
α_1	0.1	β_3	0.001
α_2	0.1	k_p	0.1
p	0.9		

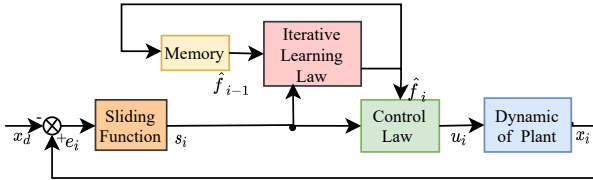


Fig. 2: Block diagram of the proposed control system.

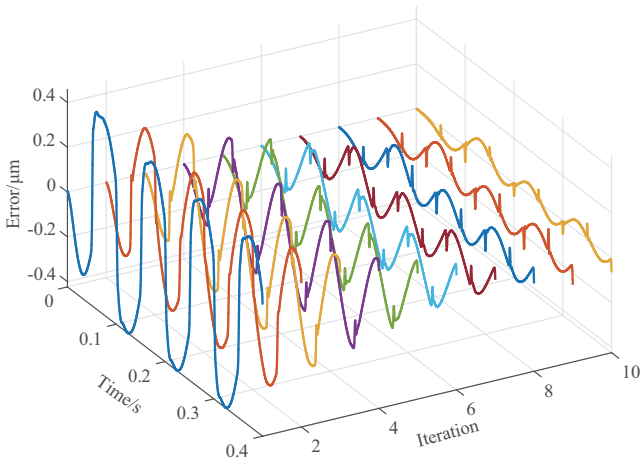


Fig. 3: Tracking errors of PIL-ITSMC for 10 iterations.

All the parameters of the controllers are demonstrated in Tab. 2. It should be noted that the parameters of ITSMC are the same for the three controllers. Furthermore, because the iterative leaning law in IL-ITSMC only contains the proportional coefficients of the sliding surface, the P-type ILC is adopted in this paper for a fair comparison. The block diagram of the proposed control system is illustrated in Fig. 2.

In the following simulations, the reference trajectory is set as $x_d(t) = 20\sin(2\pi \cdot 10 \cdot t)$ with a sampling rate 2000 Hz, and 10 iterations are conducted for PIL-ITSMC and IL-ITSMC. It should be noted that the result of first iteration is got with the pure ITSMC.

The tracking errors for the different iterations of the controllers are plotted in Fig. 3 and Fig. 4, respectively. The first iteration, i.e. ITSMC presents the worst performance, and then the tracking errors of PIL-ITSMC and IL-ITSMC are reduced during the following iterations. The root-mean-square error (e_{rms}) and maximal error (e_{max}) during iterations are given in Fig. 5, and the calculated values are listed in Tab. 3. The e_{rms} and e_{max} with ITSMC are $0.3501 \mu\text{m}$ and $0.4576 \mu\text{m}$, respectively. For the PIL-ITSMC, the tracking errors are reduced gradually from the 2nd to 10th iteration, and finally achieve the e_{rms} and e_{max} at $0.0386 \mu\text{m}$ and $0.0776 \mu\text{m}$, respectively. In contrast, the proposed IL-ITSMC reaches the e_{rms} and e_{max} at $0.0284 \mu\text{m}$ and $0.0713 \mu\text{m}$

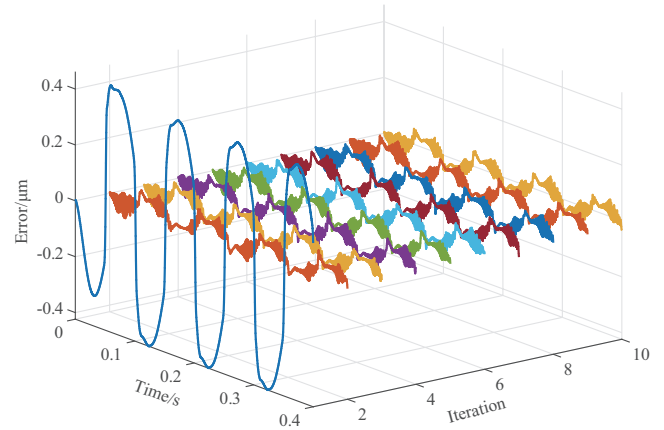


Fig. 4: Tracking errors of IL-ITSMC for 10 iterations.

Table 3: Tracking Performance of Different Controllers

Iteration	PIL-ITSMC(μm)		IL-ITSMC(μm)	
	e_{rms}	e_{max}	e_{rms}	e_{max}
1	0.3501	0.4576	0.3501	0.4576
2	0.2639	0.3778	0.0284	0.0713
4	0.1542	0.2745	0.0286	0.0760
6	0.0875	0.1738	0.0283	0.0692
8	0.0541	0.1113	0.0286	0.0763
10	0.0386	0.0776	0.0285	0.0678

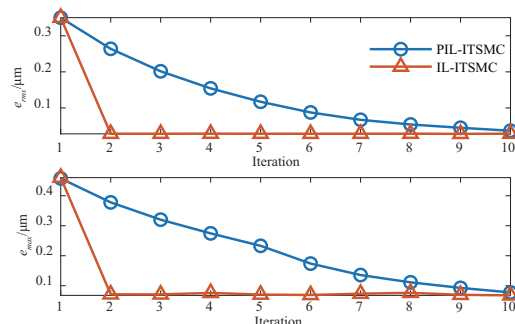


Fig. 5: e_{rms} and e_{max} of different controllers along iterations.

μm at the 2nd iteration, and retains the converged state to the 10th iteration with the e_{rms} and e_{max} at $0.0285 \mu\text{m}$ and $0.0378 \mu\text{m}$, respectively. It can be concluded that the proposed IL-ITSMC can improve the convergence speed than the traditional P-type ILC based controller. This advantage could reduce the experimental iterations significantly. The tracking performance of the three controllers at the 10th iteration are demonstrated in Fig. 6. It is evident that although the nonlinearity exists in the motion system, the tracking performance is enhanced by the proposed method, achieving the best precision.

5 Conclusions

In this paper, an iterative learning enhanced integral terminal sliding mode control is proposed for the precision motion systems suffering from various disturbances. For the

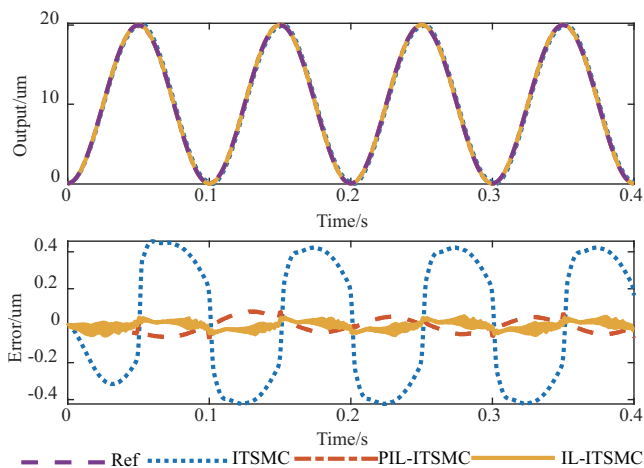


Fig. 6: Tracking performance of different controllers at the 10th iteration.

repetitive trajectory tracking commonly used in such systems, the proposed method combines the advantages of ILC and SMC-based controller to further improve the tracking performance. In order to enhance the steady-state performance and robustness to undesired disturbance, an integral terminal sliding surface and a fast reaching law are utilized to design the feedback controller. For the repetitive term caused by repetitive error and disturbance, a sliding surface based iterative learning law is integrated into the overall control scheme. Both the stability in time domain and convergence in iteration domain are proven by the Lyapunov theory. In addition, the simulations on a piezo-actuated nanopositioning system with hysteresis nonlinearities are conducted through implementing three controllers. The results show that the proposed method achieves the e_{rms} and e_{max} at $0.0285 \mu\text{m}$ and $0.0378 \mu\text{m}$, respectively, i.e. the best performance, and obtains a faster convergence speed than PIL-ITSMC.

References

- [1] M. Iwasaki, K. Seki, and Y. Maeda, "High-precision motion control techniques: A promising approach to improving motion performance," *IEEE Industrial Electronics Magazine*, vol. 6, no. 1, pp. 32–40, 2012.
- [2] X. Gao, J. Yang, J. Wu, X. Xin, Z. Li, X. Yuan, X. Shen, and S. Dong, "Piezoelectric actuators and motors: Materials, designs, and applications," *Advanced Materials Technologies*, vol. 5, no. 1, p. 1900716, 2020.
- [3] D. Sabarianand, P. Karthikeyan, and T. Muthuramalingam, "A review on control strategies for compensation of hysteresis and creep on piezoelectric actuators based micro systems," *Mechanical Systems and Signal Processing*, vol. 140, p. 106634, 2020.
- [4] S. Huang, W. Liang, and K. K. Tan, "Intelligent friction compensation: A review," *IEEE/ASME Transactions on Mechatronics*, vol. 24, no. 4, pp. 1763–1774, 2019.
- [5] M. Ming, Z. Feng, J. Ling, and X.-H. Xiao, "Hysteresis modelling and feedforward compensation of piezoelectric nanopositioning stage with a modified bouc-wen model," *Micro & Nano Letters*, vol. 13, no. 8, pp. 1170–1174, 2018.
- [6] Z. Feng, J. Ling, M. Ming, W. Liang, K. K. Tan, and X. Xiao, "Signal-transformation-based repetitive control of spiral trajectory for piezoelectric nanopositioning stages," *IEEE/ASME Transactions on Mechatronics*, vol. 25, no. 3, pp. 1634–1645, 2020.
- [7] J. Ling, M. Rakotondrabe, Z. Feng, M. Ming, and X. Xiao, "A robust resonant controller for high-speed scanning of nanopositioners: design and implementation," *IEEE Transactions on Control Systems Technology*, vol. 28, no. 3, pp. 1116–1123, 2019.
- [8] A. Sabanovic, "Variable structure systems with sliding modes in motion control—a survey," *IEEE Transactions on Industrial Informatics*, vol. 7, no. 2, pp. 212–223, 2011.
- [9] J. Ling, Z. Feng, D. Zheng, J. Yang, H. Yu, and X. Xiao, "Robust adaptive motion tracking of piezoelectric actuated stages using online neural-network-based sliding mode control," *Mechanical Systems and Signal Processing*, vol. 150, p. 107235, 2021.
- [10] J. Khawwaf, J. Zheng, R. Chai, R. Lu, and Z. Man, "Adaptive microtracking control for an underwater ipmc actuator using new hyperplane-based sliding mode," *IEEE/ASME Transactions on Mechatronics*, vol. 24, no. 5, pp. 2108–2117, 2019.
- [11] J. Zheng, H. Wang, Z. Man, J. Jin, and M. Fu, "Robust motion control of a linear motor positioner using fast nonsingular terminal sliding mode," *IEEE/ASME Transactions on Mechatronics*, vol. 20, no. 4, pp. 1743–1752, 2014.
- [12] Z. Feng, W. Liang, J. Ling, X. Xiao, K. K. Tan, and T. H. Lee, "Integral terminal sliding-mode-based adaptive integral backstepping control for precision motion of a piezoelectric ultrasonic motor," *Mechanical Systems and Signal Processing*, vol. 144, p. 106856, 2020.
- [13] Y. Pan, C. Yang, L. Pan, and H. Yu, "Integral sliding mode control: performance, modification, and improvement," *IEEE Transactions on Industrial Informatics*, vol. 14, no. 7, pp. 3087–3096, 2017.
- [14] L. Blanken, F. Boeren, D. Bruijnen, and T. Oomen, "Batch-to-batch rational feedforward control: from iterative learning to identification approaches, with application to a wafer stage," *IEEE/ASME Transactions on Mechatronics*, vol. 22, no. 2, pp. 826–837, 2016.
- [15] M. Rana, H. R. Pota, and I. R. Petersen, "Improvement in the imaging performance of atomic force microscopy: A survey," *IEEE Transactions on Automation Science and Engineering*, vol. 14, no. 2, pp. 1265–1285, 2016.
- [16] D. A. Bristow, M. Tharayil, and A. G. Alleyne, "A survey of iterative learning control," *IEEE control systems magazine*, vol. 26, no. 3, pp. 96–114, 2006.
- [17] M. M. G. Ardakani, S. Z. Khong, and B. Bernhardsson, "On the convergence of iterative learning control," *Automatica*, vol. 78, pp. 266–273, 2017.
- [18] K. L. Barton and A. G. Alleyne, "A norm optimal approach to time-varying ilc with application to a multi-axis robotic testbed," *IEEE Transactions on Control Systems Technology*, vol. 19, no. 1, pp. 166–180, 2010.
- [19] F. Boeren, A. Bareja, T. Kok, and T. Oomen, "Frequency-domain ilc approach for repeating and varying tasks: With application to semiconductor bonding equipment," *IEEE/ASME Transactions on Mechatronics*, vol. 21, no. 6, pp. 2716–2727, 2016.
- [20] J. van Zundert and T. Oomen, "On inversion-based approaches for feedforward and ilc," *Mechatronics*, vol. 50, pp. 282–291, 2018.
- [21] Y. Feng, F. Han, and X. Yu, "Chattering free full-order sliding-mode control," *Automatica*, vol. 50, no. 4, pp. 1310–1314, 2014.
- [22] Z. Zhu, Y. Xia, and M. Fu, "Attitude stabilization of rigid spacecraft with finite-time convergence," *International Journal of Robust and Nonlinear Control*, vol. 21, no. 6, pp. 686–702, 2011.